THE JOURNAL OF PHYSICAL CHEMISTRY B

ARTICLE

pubs.acs.org/JPCB

Infrared Study of the Stability and Folding Kinetics of a Series of β-Hairpin Peptides with a Common NPDG Turn

Yao Xu,[†] Deguo Du,[*,‡] and Rolando Oyola[*,§]

[†]Department of Chemistry, University of Pennsylvania, Philadelphia, Pennsylvania 19104, United States

[‡]Department of Chemistry and Biochemistry, Florida Atlantic University, Boca Raton, Florida 33431, United States

[§]Department of Chemistry, University of Puerto Rico-Humacao, Humacao, Puerto Rico 00791

ABSTRACT: The thermal stability and folding kinetics of a series of 15-residue β-hairpins with a common Type I [3:5] NPDG turn were studied using Fourier transform infrared spectroscopy (FTIR) and laser-induced temperature jump (T-jump) with infrared detection, respectively. Mutations at positions 3, 5, or 13 in the peptide sequence SEXYXNPDGTWTXTE, where X represents the position of mutation, were performed to study the roles of hydrophobic interactions in determining the thermodynamic and kinetic properties of β-hairpin folding. The thermal stability studies show a broad thermal folding/unfolding transition for all the peptides. T-jump studies indicate that these β-hairpin peptides fold in less than 2 μs. In addition, both folding and unfolding rate constants decrease with increasing strength of hydrophobic interactions. Kinetically, the hydrophobic interactions have more significant influence on the unfolding rate than the folding rate. Φ-value analysis indicates that the hydrophobic interactions between the side chains are mainly formed at the latter part of the transition-state region during the folding process. In summary, the results suggest that the formation of the native structure of these β-hairpins depends on the correct topology of the hydrophobic cluster. Besides the formation of the turn region as a key process for folding as suggested by previous studies, a hydrophobic collapse process may also play a crucial role during β-hairpin folding.

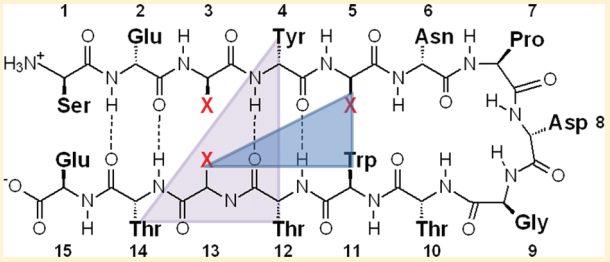

1. INTRODUCTION

Studying the factors that contribute to the folding/unfolding process of protein secondary structures should lead to better understanding of the folding mechanisms of more complex proteins. A β-sheet protein contains β-hairpin motif as a basic building block. A β-hairpin is characterized by two antiparallel strands linked by a turn or loop. Due to its small size and structural simplicity, as well as its possible role as a folding nucleus in the formation of large proteins, the β-hairpin motif has been used to study the factors that govern the conformational stability and the folding mechanism of β-sheets.[1,2] Generally, a stable β-hairpin results from an intricate interplay between several factors: (1) the intrinsic properties of the residues at the turn region to form stable β-turns, (2) the hydrophobic interactions between the side chains across the β-strands, (3) interstrand hydrogen bonds that help define and maintain the architecture of the hairpin, and (4) the polar side chain−side chain interactions.[3−9] These factors may have rather complex effects on the folding free energy landscape and the rate of β-hairpin formation.

During the past few years, numerous experimental and theoretical folding/unfolding studies have been reported for different β-hairpin sequences.[8−29] The available experimental folding time for β-hairpins spans a range of 0.8−50 μs.[30] According to the study of Muñoz et al.,[30] this small lifetime range precludes a detailed conclusion about the β-hairpin folding/unfolding mechanism. Clearly, new experimental findings continue providing valuable insight into the mechanisms of β-hairpin folding/unfolding.

Using laser-induced temperature jump (T-jump) technique, Xu et al. studied the folding mechanism of a 15-residue β-hairpin with the sequence of SESYINPDGTWTVTE (Peptide 1).[31] This peptide, designed by Santiveri et al.,[32] folds into a β-hairpin structure in aqueous solution with a type I + G1 bulge [3:5] turn involving residues Asn6, Pro7, Asp8, and Gly9. Peptide 1 shows a fast folding rate constant, approximately $(0.8\ \mu s)^{-1}$ at 300 K.[31] Its folding process encounters a low energetic barrier of ∼2 kcal·mol^{-1}. More recently, Thukral et al. reported the folding mechanism for Peptide 1 using unbiased molecular dynamics simulations.[33] According to their results, the turn is the major determinant in initiating the folding process, followed by the cooperative formation of the interstrand hydrogen bonds and the side-chain packing. Moreover, the transition to the folded state from fully unstructured conformations is carried out through a partially structured conformation involving a non-native (ESYI) turn. This transient intermediate structure leads to the formation of the native (NPDG) turn and consequently triggers the folding of the peptide into the native state.[33]

Received: May 19, 2011
Revised: November 11, 2011
Published: December 02, 2011

Table 1. Peptide Sequences with a Common NPDG Turn: SEXYXNPDGTWTXTE

	position X		
	3	5	13
Peptide 1	S	I	V
NPDGm1	I	S	V
NPDGm2	I	W	V
NPDGm3	I	W	W

In this work, we report the thermal stability and folding/unfolding kinetics of a series of β-hairpins with the common turn sequence, NPDG (Table 1). As noted by Olsen et al., the folding kinetics of the β-hairpins that have been studied experimentally primarily contain [4:4] or [2:2] type turns.[34] Until now, little dynamic information about [3:5] turns is available. For this reason, three β-hairpin peptides, NPDGm1, NPDGm2, and NPDGm3 (Table 1), were studied both thermodynamically and kinetically. NPDGm1 is originally designed by Santiveri et al.[32] and it includes a double mutation of Peptide 1 at positions 3 and 5. NPDGm2 differs from NPDGm1 by the mutation of S5W. NPDGm3 differs from NPDGm2 by the mutation of V13W, thus increasing the hydrophobic interactions due to the presence of Trp−Trp side chain interactions. In order to explore the folding/unfolding mechanisms of these β-hairpin sequences, we measured the thermal stabilities of the peptides using FTIR and circular dichroism (CD) spectroscopies while the folding/unfolding kinetics were measured using nanosecond laser-induced T-jump with IR probe. On the basis of our experimental results, we systematically studied the contribution of the side-chain interactions to the folding/unfolding process of these β-hairpin peptides.

2. EXPERIMENTAL METHODS

2.1. Sample Preparation. All β-hairpins were prepared using standard solid-phase peptide synthesis on Fmoc-Glu(OBut)-Wang resin (Model PS3, PTI Instruments, AZ). The crude samples were purified to homogeneity by reverse-phase HPLC and characterized by MALDI-MS. The residual trifluoroacetic acid (TFA) from peptide synthesis and purification was removed by lyophilization against 0.1 M DCl/D_2O several times. For both equilibrium and time-resolved IR experiments, the peptides were dissolved in 50 mM phosphate buffer in D_2O (pH* = 7) and the final concentrations ($\sim$ 3 mM) were determined by Trp absorption at 280 nm.

2.2. Equilibrium Measurements. Fourier transform infrared spectroscopy spectra were collected on a Nicolet Magna-IR 860 spectrometer using 1 cm^{-1} spectral resolution.[31] A CaF_2 sample cell was divided into two compartments using a 52 μm Teflon spacer to allow the measurements of both sample and background (pH* = 7, 50 mM phosphate buffer) under identical conditions. Temperature was controlled using a circulator bath with $\pm$ 0.2 °C precision. A translation stage was used to allow movement of both the sample and the reference in and out of the IR beam alternatively to correct the slow instrument drift, and each time a spectrum corresponding to an average of 256 scans was collected.

Circular dichroism thermal melting curves were obtained on an Aviv 62A DS spectropolarimeter (Aviv Associates, NJ) with a 1 mm sample holder. The peptide concentration was about 50 μM in 50 mM phosphate buffer solution (pH = 7). The folding equilibrium constant ($K_{eq}(T)$) was obtained by fitting the mean residue ellipticities ($\theta(T)$) at 229 nm over a range of temperatures according to an apparent two-state model, eqs 1−3.

$$\theta(T) = \frac{\theta_U(T) + K_{eq}(T)\theta_F(T)}{1 + K_{eq}(T)} \quad (1)$$

$$K_{eq}(T) = \exp(-\Delta G/RT) \quad (2)$$

$$\Delta G(T) = \Delta H_m + \Delta C_p(T - T_m) - T[\Delta S_m + (\Delta C_p)\ln(T/T_m)] \quad (3)$$

where $\theta_F(T)$ is the pretransition baseline, and $\theta_U(T)$ is the post-transition baseline, $T_m = \Delta H_m/\Delta S_m$ is the thermal melting temperature, ΔH_m and ΔS_m is the enthalpy and entropy change at T_m, respectively, and ΔC_p is the heat capacity change associated with unfolding, which has been assumed here to be temperature independent. In the current study, both $\theta_F(T)$ and $\theta_U(T)$ were treated as a linear function of temperature, i.e., $\theta_F(T) = a + bT$ and $\theta_U(T) = c + dT$, where a, b, c, and d are constants defined as global parameters during the fit. The fitting variables are allowed to change without constraints during the nonlinear regression. The resulting ΔC_p value is close to zero for NPDGm1 in agreement with the results of Santiveri et al.[32] In this case, we report a ΔC_p value of zero. A similar situation was observed in the thermal unfolding transition of NPDGm1 in the FTIR experiments.

2.3. Time-Resolved T-Jump Infrared Measurements. The laser-induced T-jump infrared setup used in this study has been reported in detail elsewhere.[31] Briefly, the 3 ns, 10 mJ, 1.9 μm, and 10 Hz T-jump pulse was generated via Raman shifting the Nd:YAG fundamental, 1064 nm, in H_2 gas pressurized at 750 psi. A continuous wave (CW) lead-salt infrared diode laser served as the probe. Transient absorbance changes of the probe induced by the T-jump pulses were detected by a 50 MHz mercury cadmium telluride (MCT) detector. Digitization of the signal was accomplished by a Tektronix TDS 3052 digital oscilloscope. As in the FTIR measurements, a sample cell with dual compartments was used to allow the separate measurements of the sample and the reference (D_2O phosphate buffer, pH* 7) under identical conditions. The measurements on reference ($\Delta OD_r(\Delta T,t)$) provide information for both the background subtraction and T-jump amplitude determination. Calibration of the T-jump amplitude was achieved by using the T-jump induced absorbance change of the D_2O buffer solution at the probing frequency, $\Delta OD_r(\Delta T,\nu)$, and the following equation: $\Delta OD_r(\Delta T,\nu) = a(\nu)^*\Delta T + b(\nu)^*\Delta T^2$, where ΔT corresponds to the difference between the final (T_f) and initial (T_i) temperatures, and $a(\nu)$ and $b(\nu)$ are the fitting parameters determined by analyzing the temperature dependence of the FTIR spectra of the D_2O buffer solution under equilibrium conditions measured at different temperatures.[21,22,31] The observed sample transient signal ($\Delta OD_s(\Delta T,\nu)$) contains contributions from both sample and solvent. To correct these transients and obtain only the sample contribution, each sample transient signal was subtracted by the reference signal under identical experimental conditions.

3. RESULTS

3.1. Equilibrium Infrared Spectroscopy. The thermal unfolding of NPDGm1, NPDGm2, and NPDGm3 was studied by

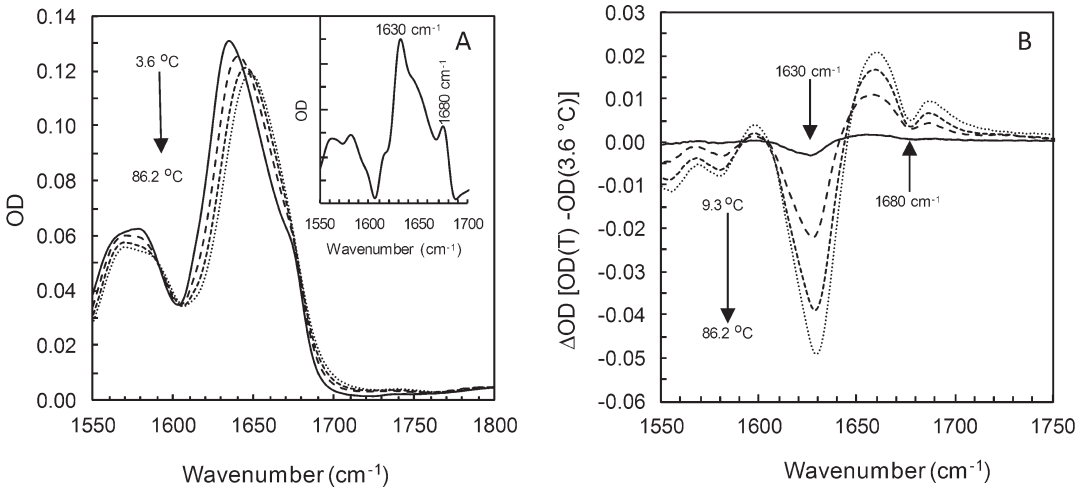

Figure 1. (A) Equilibrium FTIR spectra of NPDGm3 in D_2O phosphate buffer (pH* 7.0) at 3.6 °C (solid line), 38.4 °C (long dashed), 62.4 °C (medium dashed), and 86.2 °C (short dashed). Inset: Fourier self-deconvolution spectrum at 3.6 °C with $k = 2$ and full width half-maximum =18 cm^{-1}. (B) Difference FTIR spectra that were generated by subtracting the spectrum collected at the lowest temperature (3.6 °C) from those obtained at 9.3 °C (solid line), 38.4 °C (long dashed), 62.4 °C (medium dashed), and 86.2 °C (short dashed).

FTIR spectroscopy using the amide I′ absorption band as a conformational probe. This band has been shown to be sensitive to protein secondary structure.[35] The FTIR spectra in the amide I′ band region as a function of temperature for NPDGm3 is shown in Figure 1A. The broad amide I′ band is subject to resolution enhancement using Fourier self-deconvolution (FSD) (inset of Figure 1A). At low temperature (3.6 °C), the spectrum shows characteristic antiparallel β-sheet bands centered at 1630 and 1680 cm^{-1}. These vibrational bands are mainly due to interstrand transition dipole couplings, and through-bond and through-space vibrational couplings between the amide carbonyls.[36,37] The quantitative differences of the position and the intensity of the two coupled bands are due to the twist angle and distance between the two β-strands. For NPDGm1 and NPDGm2, the FSD analysis shows lower intensity bands at 1630 and 1680 cm^{-1} (data not shown). The thermal reversibility of the FTIR spectra (data now shown) demonstrates that the thermal folding/unfolding of these peptides is reversible. In addition, the absence of a sharp peak at 1618 cm^{-1}, the characteristic IR absorbance band of aggregated β-sheet species,[38] suggests that the peptides do not form aggregates under the current experimental conditions.

Quantitative decomposition of the amide I′ IR absorption spectrum into its components is difficult because of the high overlapping of the bands. It has been shown that the high-frequency component of β-sheets in the region of 1680 cm^{-1} can be used to characterize the thermal unfolding transition of β-hairpins quantitatively as the band area is proportional to the folded population of β-hairpin peptides.[22,31,39] To fulfill this goal, the FTIR difference spectra are used in order to amplify the change of the characteristic vibrational component at ~1680 cm^{-1} and a global fitting procedure is applied to obtain the thermodynamic parameters as described previously by Wang et al. in detail.[39] The FTIR difference spectra are generated by subtracting the spectrum collected at the lowest reference temperature, OD(T_R,ν), from spectra collected at higher temperatures, OD(T,ν), as shown in Figure 1B. The difference spectra show bands at approximately 1630 and 1680 cm^{-1} that lose intensity as temperature increases (Figure 1B), indicating the decrease of the folded β-hairpin population with increasing temperature. Moreover, an increase

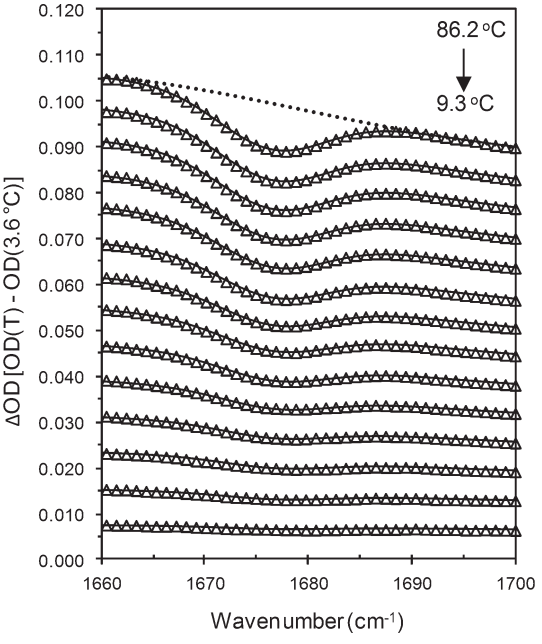

Figure 2. Difference FTIR spectra (△) of NPDGm3 in D_2O phosphate buffer (pH* 7.0) in the high-frequency region. These spectra were generated by subtracting the FTIR collected at 3.6 °C from those collected at higher temperatures and adding an offset for clarity purpose. Solid lines are fit to a Gaussian function plus a nonlinear baseline term consisting of a Gaussian and linear function. The dotted line corresponds to the baseline of the difference spectrum at 86.2 °C.

of band intensity with maximum at 1660 cm^{-1} in the difference spectra is observed, which indicates the increase of the unfolded population at higher temperatures. Global fitting of the difference spectra in the 1680 cm^{-1} region using a Gaussian function plus a nonlinear baseline that consists of a broad Gaussian and a linear background allows the determination of the integrated area of the ~1680 cm^{-1} band at different temperatures,[21,31,39] as shown in Figure 2. The integrated area of the ~1680 cm^{-1} band, which is proportional to the folded β-hairpin population, at different

temperatures are analyzed using an apparent two-state model to obtain the thermodynamic parameters of β-hairpin unfolding.[21,31,39] The fitting results for each mutant peptide are shown in Figure 3, and the thermodynamic parameters are summarized in Table 2.

As shown in Figure 3, the thermal unfolding of NPDGm1 exhibits a broad transition, while higher transition cooperativity is observed for NPDGm2 and NPDGm3. The folded population of NPDGm1, NPDGm2, and NPDGm3 at 298 K is estimated to be 35, 54, and 68%, respectively (inset of Figure 3). The increase of folded population at 298 K is accompanied by an increase of the thermal stability (Table 2). It is expected that the stability of the β-hairpin structure increases by introducing hydrophobic Trp residues into the sequence. Indeed, the mutation of S5W in NPDGm1 results in the increase of T_m from ~10 to ~30 °C, a value similar to that of Peptide 1. Mutation of V13W in NPDGm2 increases T_m further to ~37 °C. These results are consistent with the fact that incorporating Trp residues provides strong side-chain hydrophobic interactions. Similar hydrophobic substitution effects were observed in trpzip β-hairpin derivatives.[21] In addition, the relative strength of the hydrophobic interaction is also indicated by the values of ΔC_p. For example, the nearly zero value of ΔC_p for NPDGm1 ($\sim 0 \pm 62$ J·mol^{-1}·K^{-1}) suggests that the folded structure of this peptide does not have a tightly packed hydrophobic core, consistent with the null heat capacity change obtained by other studies.[32,40] Additionally, the higher ΔC_p values for NPDGm2 and NPDGm3 indicate the stronger hydrophobic interactions in these two peptides.

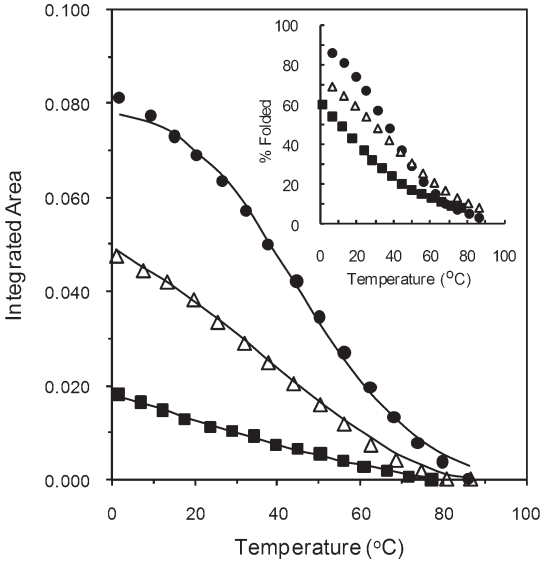

Figure 3. Integrated area of the 1680 cm^{-1} band vs temperature for NPDGm1 (■), NPDGm2 (△), and NPDGm3 (●). The solid lines correspond to the best fit of the data to a two-state model. Inset: the temperature dependence of the folded population of the three peptides. The folded population (f) was calculated from the equilibrium constant at temperature T using the relation $K_{eq}(T) = f/(1 - f)$. The thermodynamic parameters are summarized in Table 2.

3.2. CD Thermal Studies. Although β-hairpin peptides usually do not show a CD signal that is reliable to monitor the thermal transitions, the buried aromatic side chains may give rise to a pronounced positive CD peak at ~229 nm, which can be used to obtain the thermodynamic transition curve. Unlike Peptide 1 and NPDGm1, NPDGm2 and NPDGm3 show a positive intensity band at around 229 nm (data not shown) arising from the excitonic coupling between the paired Trp side chains.[41,42] Moreover, the thermal unfolding transition was followed by monitoring the CD signals at 229 nm as a function of temperature. The thermodynamic parameters from a two-state model are very similar to those obtained from IR analysis (Table 2).

3.3. T-Jump IR Relaxation Kinetics. The relaxation kinetics of the NPDG peptides was measured by employing T-jump technique with IR absorption. The T-jump experiment allows the measurement of relaxation rate constants after perturbation of the equilibrium of the system by a rapid increase in temperature. A diode laser beam at 1634 cm^{-1} is used to probe the decreasing absorption intensity due to the loss of β-sheet structure. As an example, the relaxation kinetic trace for NPDGm3 probed at 1634 cm^{-1} induced by a T-jump from 18.5 to 28.1 °C and background corrected is shown in Figure 4. The kinetic trace shows a negative absorbance change because the equilibrium is shifted to a higher unfolded population after the T-jump.

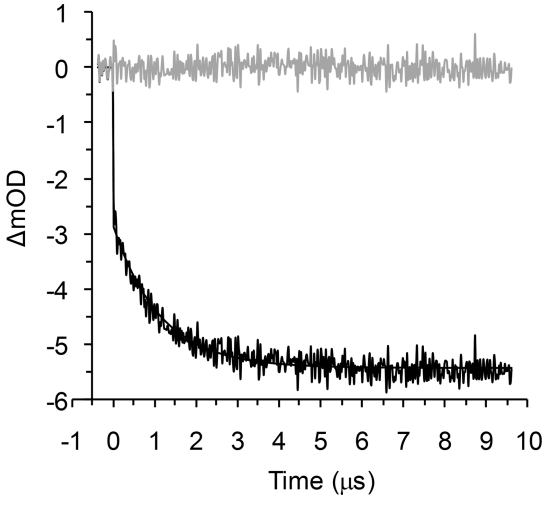

Figure 4. A representative relaxation kinetic trace (black) probed at 1634 cm^{-1} for NPDGm3 in 50 mM phosphate buffer (pH* 7.0) with a T-jump from 18.5 to 28.1 °C. The solid line is the fit to the following function, $\Delta OD(t) = A[1 - B \exp(-t/\tau)]$ with values of $A = -0.00544$, $B = 0.475$, and $\tau_{obs} = 1.13$ μs. Residual analysis of the fit (gray) is also shown.

Table 2. Thermodynamic Unfolding Parameters Obtained from Equilibrium IR and CD Measurements

peptide	ΔH_m (kJ·mol^{-1})	ΔS_m (J·mol^{-1}·K^{-1})	ΔC_p (J·mol^{-1}·K^{-1})	T_m (°C)
Peptide 1[a]	27.8	92	~0	29.1
NPDGm1	27 ± 3	97 ± 9	~0	10.3
NPDGm2	29 ± 3 (30 ± 3)[b]	96 ± 8 (98 ± 10)	356 ± 36 (355 ± 36)	29.8 (32.3)
NPDGm3	48 ± 5 (54 ± 5)	155 ± 20 (173 ± 16)	421 ± 40 (477 ± 36)	37.3 (39.4)

[a] Taken from Xu et al.[31] [b] Values in parentheses are from CD measurements.

dx.doi.org/10.1021/jp2046867 |J. Phys. Chem. B 2011, 115, 15332–15338

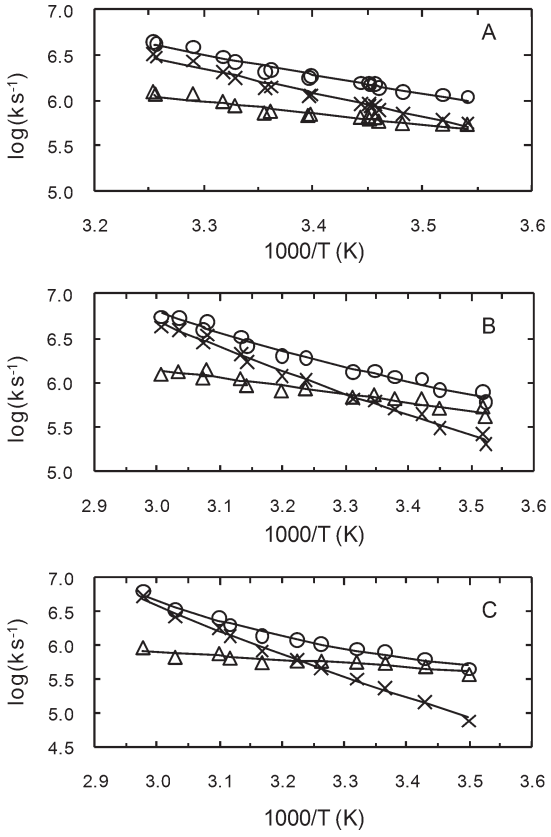

Figure 5. Arrhenius plots of the observed relaxation (○), folding (△), and unfolding (×) rate constants of (A) NPDGm1, (B) NPDGm2, and (C) NPDGm3. The folding and unfolding rate constants are calculated by using the $K_{eq}(T)$ determined from the FTIR measurements (Table 2). Both the folding and unfolding rate constants are fitted using the following equation: $\ln(k) = \ln(D) - \Delta G^{\ddagger}/RT$, where D is a constant and set to 10^{10} s^{-1}, and $\Delta G^{\ddagger}$ is the free energy of activation of folding or unfolding. The best fits are shown as solid lines. The top solid line represents the calculated relaxation rate constants which equal to the sum of the fitting values of the folding and unfolding rate constants.

The relaxation decay exhibits two distinct phases. The fast phase is instrumentation-limited, likely due to temperature-induced spectral changes, such as shift and broadening, and/or imperfect background subtraction, whereas the slow phase can be modeled using a single exponential function. The observation of first-order relaxation kinetics for these β-hairpins indicates that their folding process from thermally denatured state can be described by a two-state model. The observed relaxation rate constant (k_{obs}) has contributions from both folding (k_f) and unfolding (k_u) rate constants. Each rate constant can be further determined using the following relationships for a two-state model: $k_{obs} = k_f + k_u$ and $K_{eq}(T) = k_f/k_u$, where $K_{eq}(T)$ is the equilibrium constant at temperature T, which is calculated from the equilibrium FTIR measurements.

The temperature dependence of k_f and k_u shown in Figure 5 is represented as the Arrhenius plots. To reveal the intrinsic energetic barriers associated with the folding and unfolding, we fit the temperature-dependent rate constants of both folding and unfolding simultaneously using the following equation: $\ln(k) = \ln(D) - \Delta G^{\ddagger}/RT$, where D is a constant, and $\Delta G^{\ddagger}$ is the temperature-dependent free energy of activation. The free energy of activation for folding or unfolding is determined using an equation

Table 3. Folding and Unfolding Dynamic Parameters at 25°C

peptide	$\Delta H_f^{\ddagger}$ (kJ·mol^{-1})	$\Delta H_u^{\ddagger}$ (kJ·mol^{-1})	k_{obs}^{-1} (μs)	k_f^{-1} (μs)	k_u^{-1} (μs)
Peptide 1[a]	8.36	36.4		0.76	0.92
NPDGm1	22 ± 2	51 ± 1	0.41 ± 0.03	1.19 ± 0.08	0.62 ± 0.04
NPDGm2	16 ± 1	44 ± 4	0.82 ± 0.03	1.51 ± 0.05	1.80 ± 0.07
NPDGm3	10 ± 1	59 ± 5	1.36 ± 0.05	1.98 ± 0.07	4.34 ± 0.21

[a] Taken from Xu et al.[31]

analogous to eq 3, i.e., $\Delta G^{\ddagger} = \Delta H_m^{\ddagger} + \Delta C_p^{\ddagger}(T - T_m) - T[\Delta S_m^{\ddagger} + \Delta C_p^{\ddagger} \ln(T/T_m)]$, where T_m is thermal melting temperature, $\Delta H_m^{\ddagger}$, $\Delta S_m^{\ddagger}$, and $\Delta C_p^{\ddagger}$ are the enthalpy, entropy, and heat capacity of activation at T_m, respectively.

The best fit of the temperature dependence of the folding and unfolding rate constants yields a relatively small folding activation enthalpy ($\Delta H_f^{\ddagger}$, Table 3). The results suggest that these β-hairpins encounter a very low energy barrier to form their native structure from the thermally denatured state, indicating that the folding of these β-hairpins is largely entropically controlled, consistent with our previous studies.[21,31,43]

4. DISCUSSION

A wealth of information has been obtained during the past few years on the thermal stability and folding/unfolding kinetics of β-hairpin peptides.[1−9,21,43] Here we present a study of the thermal stability and folding dynamics of a series of 15-residue β-hairpin peptides with a common NDPG turn. These NPDG β-hairpins contain a [3:5] Type I β-turn with a G1 β-bulge. Peptide 1 is one of the NPDG β-hairpins whose thermal stability and folding/unfolding dynamics have been reported. As previously suggested,[31] Peptide 1 does not form a well-packed hydrophobic cluster relative to other commonly studied β-hairpins.[31] A plausible reason is that the NPDG turn induces a high strand twist which in consequence leads to the diminished diagonal and interstrand side-chain interactions. Nonetheless, Peptide 1 still shows characteristic nuclear Overhauser effect (NOE) signals between hydrophobic residues at positions 5, 11, and 13 on the same side of the β-hairpin, and positions 4, 12, and 14 on the other side of Peptide 1 (Jiménez, M. A., personal communication). Modifications of the hydrophobic region in the Peptide 1 allow us to determine the effect of the hydrophobic interactions on the thermal stability and folding/unfolding dynamics of the β-hairpins with NPDG turn. The first modification consists of a double mutation, S3I and I5S, by exchanging the residues at positions 3 and 5 in Peptide 1. This mutation causes a decrease in the thermal stability of approximately 20 °C (NPDGm1). Thus, the formation of a hydrophobic interaction between the residues 5, 11, and 13 seems to play a key role in determining the thermal stability of Peptide 1. This is in agreement with the observed NOE signals between the residues at positions 5, 11, and 13 which locate on the same side of the peptide. It is expected that if the hydrophobic core is re-established by introducing a nonpolar amino acid residue at position 5, the stability of the native state of β-hairpin should increase accordingly. Consistent with this expectation, a single mutation of S5W in NPDGm1 results in the recovering of the thermal stability. In addition, the presence of Trp at position 5 results in a higher ΔC_p which can be attributed to W5−W11−V13 side chain−side chain interactions. Mutation of V13W in NPDGm2 further leads to a 7 °C increase in thermal stability with an accompanying higher ΔC_p.

The folding kinetics of the β-hairpins were studied by the T-jump technique in conjunction with infrared spectroscopy. The kinetic folding rates of these peptides are faster than those for most of the other commonly studied β-hairpins with similar size.[30] The fast folding rate may arise from the rigidity of the Pro residue at the turn region, which restricts the number of conformations available to form the folding nucleus and helps to decrease the entropy cost of the turn formation by constraining the flexibility of the loop. Other factors such as the length of the strands and the relative position of hydrophobic clusters to the turn could also play a role in the folding kinetics of β-hairpins. For example, Muñoz et al. reported an ubiquitin β-hairpin derivative containing the NPDG turn with a folding time of 50 μs.[30] The authors attributed the observed long folding time to the farther distance of the hydrophobic cluster relative to the turn. Interestingly, the thermal stability of this derivative is similar to those of Peptide 1 and NPDGm2.

Comparisons between the folding/unfolding rates of these β-hairpins reveal that mutations in the hydrophobic cluster region result in different effects on the folding and unfolding kinetics. As shown in Table 3, at 298 K, the folding rate slightly decreases from NPDGm1 to NPDGm3 by a factor of 1.7, while the unfolding rate decreases by a factor of 7. These results suggest that the major kinetic role of the hydrophobic interactions is to prevent the β-hairpin from unfolding. The stability of a β-hairpin native conformation increases with increasing hydrophobic interactions primarily by decreasing its unfolding rate. This is in agreement with other early conclusions based on the kinetic studies of a series of tryptophan zipper β-hairpins.[21,43] On the other hand, although NPDGm1, NPDGm2, and NPDGm3 contain the same turn, the small but noticeable decrease of the folding rate is observed accompanied by the increase of hydrophobic interactions. The difference between the observed folding rates may arise from the quick formation of the collapsed structures with non-native topology, which need to be rearranged (i.e., breaking non-native hydrophobic interactions) over an energetic barrier to reach the correctly folded native state.

A convenient overview of the hydrophobic interactions on folding kinetics of the β-hairpins is provided by Φ-value analysis.[43] Φ-value represents the mutation-induced change of the transition-state free energy relative to the change of the equilibrium free energy of folding. If the mutation destabilizes the transition state as much as the folded state, Φ equals 1. If the mutation has no effect on transition state, Φ is zero. At 25 °C, a single mutation of S5W in NPDGm1 leads to a small Φ value of ~ -0.27, suggesting that the native contacts involving the residue at position 5 are not developed well at the folding transition state. A more hydrophobic residue at this position slightly destabilizes the transition state while it stabilizes the native conformation dramatically. It is worth noting that this position is located at the hydrophobic cluster region closer to the turn. These results suggest that the formation of the well-packed hydrophobic cluster is mainly located after the transition state along the folding pathway, that is, the downhill side from the barrier to the folded state, in agreement with other studies.[21,43]

The folding barrier from the thermally denatured state to native state can also be viewed, based on the energy landscape theory, as a rather broad and continuous transition with fluctuations.[44−46] It has been shown that the roughness of the folding energy landscape increases as folding proceeds to the native state.[47,48] The roughness can arise from various factors, such as non-native interactions or native interactions in the wrong topology, side-chain steric effects, etc. Increasing hydrophobic interactions between the residue side chains may raise the roughness of the free energy profile, resulting in a slower folding and unfolding kinetics.[49] Since the formation of the hydrophobic interaction is located after the transition-state region along the folding free energy surface, it very likely provides a more significant influence on the unfolding rate constant than that on the folding rate constant of β-hairpins, as suggested by our current results.

Santiveri et al.[32] proposed a folding mechanism of Peptide 1 by studying the T_m values obtained from subsets of protons signal at different peptide regions. This mechanism, similar to the zipper model,[16,17] states that the turn formation is the initial step followed by interstrand hydrogen bonding and hydrophobic core formation in parallel fashion.[32] Molecular dynamics simulations of Peptide 1 reported by Thukral et al.[33] showed that a non-native turn, composed of residues 2 to 5 (ESYI), is a transient intermediate. This transient intermediate leads to the native (NPDG) turn formation, triggering the hydrogen and hydrophobic interactions that result in the formation of the folded structure of the β-hairpin.[33] Both of the proposed mechanisms indicate the importance of turn formation in the folding process. However, numerous turn structures may be formed during the conformational search and not all the turns provide the correct topology to trigger the folding of β-hairpin. The favorable turn should provide the correct alignment of the interstrand hydrogen bonds and/or the side chain−side chain interactions. Therefore, exchanging positions of the Ser3 and Ile5 in Peptide 1 not only disturbs the hydrophobic core composed of residues 5, 11, and 13 in the native state of the molecule, but also may hamper the formation of the non-native ESYI turn. These effects, taken together, may contribute to the faster folding kinetics of Peptide 1 compared to that of NPDGm1.

It is worth noting that our analysis is based on a two-state model. One of the phenomena for a multistate folding process of proteins is the observation of bi- or multiexponential relaxation kinetics which is related to the presence of reaction intermediates and/or multiple reaction pathways. The single thermal unfolding transition and single-exponential relaxation kinetics observed in our studies suggest that, with the methods used in the current work, no distinguishable transient intermediates are identified during folding of these peptides. To distinguish between two-state or multistate models, a conformational probe that provides structural information of local regions in the peptide is desired.[23,32] Interestingly, Hauser et al.[23] reported the equilibrium and dynamic studies of several tryptophan zipper β-hairpin derivatives by using ^{13}C isotopic labeling. Their experimental approach provides detailed structural information during folding of those peptides because it probes the conformational change in specific regions of the peptides. Their results reveal a multistate dynamic and equilibrium behavior of the folding/unfolding mechanism for tryptophan zipper derivatives. The authors concluded that the unfolding of the β-hairpins progresses from the termini and turn toward the center of the strands, meaning that the folding is initiated by a hydrophobic collapse.[23] The results presented in our work provide insight into the roles of the hydrophobic cluster interactions in the folding and unfolding mechanism of the NPDG β-hairpin peptides in agreement with previous studies.[21,31,43] Here, our data indicate that the hydrophobic interactions not only strongly influence the unfolding rate but also play an important role in determining the folding rate of β-hairpins.

5. CONCLUSION

The present work systematically studies the thermal stability and folding kinetics of a series of 15-residue β-hairpin peptides with a common β-turn NPDG. The results show that all the studied peptides undergo a fairly broad thermal unfolding transition that can be described by a two-state model. These peptides fold within 2 μs and are among the β-hairpins with the fastest folding rates reported up to now. Our results demonstrate that the major kinetic role of the hydrophobic interactions in these peptides is to affect their unfolding process. The presence of strong hydrophobic interactions in the β-hairpin peptide decreases the unfolding rate dramatically, therefore preventing the unfolding of the β-hairpin from its native structure. Moreover, our results suggest that the formation and rearrangement of the hydrophobic clusters in the folding process of these β-hairpins also play an important role in determining the folding rate of the peptides.

AUTHOR INFORMATION

Corresponding Author

*Tel.: (561) 297-3390 (D.D.); 787-850-9387 (R.O.). Fax: (561) 297-2759 (D.D.); 787-850-9422 (R.O.). E-mail: ddu@fau.edu (D.D.); rolando.oyola@upr.edu (R.O.).

ACKNOWLEDGMENT

This project has been supported in part by NIH-NCRR-INBRE (P20RR016470). We thank Dr. Feng Gai for his support of this work.

REFERENCES

(1) Hughes, R. M.; Waters, M. L. *Curr. Opin. Struct. Biol.* **2006**, *16*, 514–524.
(2) Sharpe, T.; Jonsson, A. L.; Rutherford, T. J.; Daggett, V.; Fersht, A. R. *Protein Sci.* **2007**, *16*, 2233–2239.
(3) Blanco, F.; Ramirez-Alvarado, M.; Serrano, L. *Curr. Opin. Struct. Biol.* **1998**, *8*, 107–111.
(4) Kobayashi, N.; Honda, S.; Yoshii, H.; Munekata, E. *Biochemistry* **2000**, *39*, 6564–6571.
(5) Cochran, A. G.; Skelton, N. J.; Starovasnik, M. A. *Proc. Natl. Acad. Sci. U.S.A.* **2001**, *98*, 5578–5583.
(6) Espinosa, J. F.; Syud, F. A.; Gellman, S. H. *Protein Sci.* **2002**, *11*, 1492–1505.
(7) Dyer, R. B.; Maness, S. J.; Peterson, E. S.; Franzen, S.; Fesinmeyer, R. M.; Andersen, N. H. *Biochemistry* **2004**, *43*, 11560–11566.
(8) Fesinmeyer, R. M.; Hudson, F. M.; Andersen, N. H. *J. Am. Chem. Soc.* **2004**, *126*, 7238–7243.
(9) Lewandowska, A.; Oldziej, S.; Liwo, A.; Scheraga, H. A. *Biophys. Chem.* **2010**, *151*, 1–9.
(10) Bauer, M. C.; Xue, W. F.; Linse, S. *Int. J. Mol. Sci.* **2009**, *10*, 1552–1566.
(11) Bonomi, M.; Branduardi, D.; Gervasio, F. L.; Parrinello, M. *J. Am. Chem. Soc.* **2008**, *130*, 13938–13944.
(12) Evans, D. A.; Wales, D. J. *J. Chem. Phys.* **2004**, *121*, 1080–1090.
(13) Huyghues-Despointes, B. M.; Qu, X.; Tsai, J.; Scholtz, J. M. *Proteins* **2006**, *63*, 1005–1017.
(14) Lewandowska, A.; Oldziej, S.; Liwo, A.; Scheraga, H. A. *Proteins* **2010**, *78*, 723–737.
(15) Lewandowska, A.; Oldziej, S.; Liwo, A.; Scheraga, H. A. *Biopolymers* **2010**, *93*, 469–480.
(16) Muñoz, V.; Thompson, P. A.; Hofrichter, J.; Eaton, W. A. *Nature* **1997**, *390*, 196–199.
(17) Muñoz, V.; Henry, E. R.; Hofrichter, J.; Eaton, W. A. *Proc. Natl. Acad. Sci. U.S.A.* **1998**, *95*, 5872–5879.
(18) Shao, Q.; Yang, L.; Gao, Y. Q. *J. Chem. Phys.* **2009**, *130*, 195104.
(19) Skwierawska, A.; Makowska, J.; Oldziej, S.; Liwo, A.; Scheraga, H. A. *Proteins* **2009**, *75*, 931–953.
(20) Wei, Y.; Huyghues-Despointes, B. M.; Tsai, J.; Scholtz, J. M. *Proteins* **2007**, *69*, 285–296.
(21) Du, D.; Zhu, Y.; Huang, C. Y.; Gai, F. *Proc. Natl. Acad. Sci. U.S.A.* **2004**, *101*, 15915–15920.
(22) Gai, F.; Du, D.; Xu, Y. *Methods Mol. Biol.* **2007**, *350*, 1–20.
(23) Hauser, K.; Krejtschi, C.; Huang, R.; Wu, L.; Keiderling, T. A. *J. Am. Chem. Soc.* **2008**, *130*, 2984–2992.
(24) Huang, R.; Wu, L.; McElheny, D.; Bour, P.; Roy, A.; Keiderling, T. A. *J. Phys. Chem. B* **2009**, *113*, 5661–5674.
(25) Narayanan, R.; Pelakh, L.; Hagen, S. J. *J. Mol. Biol.* **2009**, *390*, 538–546.
(26) Shao, Q.; Wei, H.; Gao, Y. Q. *J. Mol. Biol.* **2010**, *402*, 595–609.
(27) Wu, L.; McElheny, D.; Huang, R.; Keiderling, T. A. *Biochemistry* **2009**, *48*, 10362–10371.
(28) Xiao, Y.; Chen, C.; He, Y. *Int. J. Mol. Sci.* **2009**, *10*, 2838–2848.
(29) Yang, L.; Shao, Q.; Gao, Y. Q. *J. Phys. Chem. B* **2009**, *113*, 803–808.
(30) Muñoz, V.; Ghirlando, R.; Blanco, F. J.; Jas, G. S.; Hofrichter, J.; Eaton, W. A. *Biochemistry* **2006**, *45*, 7023–7035.
(31) Xu, Y.; Oyola, R.; Gai, F. *J. Am. Chem. Soc.* **2003**, *125*, 15388–15394.
(32) Santiveri, C. M.; Santoro, J.; Rico, M.; Jiménez, M. A. *J. Am. Chem. Soc.* **2002**, *124*, 14903–14909.
(33) Thukral, L.; Smith, J. C.; Daidone, I. *J. Am. Chem. Soc.* **2009**, *131*, 18147–18152.
(34) Olsen, K. A.; Fesinmeyer, R. M.; Stewart, J. M.; Andersen, N. H. *Proc. Natl. Acad. Sci. U.S.A.* **2005**, *102*, 15483–15487.
(35) Arrondo, J. L.; Muga, A.; Castresana, J.; Goni, F. M. *Prog. Biophys. Mol. Biol.* **1993**, *59*, 23–56.
(36) Wi, S.; Pancoska, P.; Keiderling, T. A. *Biospectroscopy* **1998**, *4*, 93–106.
(37) Baumruk, V.; Pancoska, P.; Keiderling, T. A. *J. Mol. Biol.* **1996**, *259*, 774–791.
(38) Maness, S. J.; Franzen, S.; Gibbs, A. C.; Causgrove, T. P.; Dyer, R. B. *Biophys. J.* **2003**, *84*, 3874–3882.
(39) Wang, T.; Xu, Y.; Du, D.; Gai, F. *Biopolymers* **2004**, *75*, 163–172.
(40) Santiveri, C. M.; Santoro, J.; Rico, M.; Jiménez, M. A. *Protein Sci.* **2004**, *13*, 1134–1147.
(41) Wu, L.; McElheny, D.; Takekiyo, T.; Keiderling, T. A. *Biochemistry* **2010**, *49*, 4705–4714.
(42) Takekiyo, T.; Wu, L.; Yoshimura, Y.; Shimizu, A.; Keiderling, T. A. *Biochemistry* **2009**, *48*, 1543–1552.
(43) Du, D.; Tucker, M. J.; Gai, F. *Biochemistry* **2006**, *45*, 2668–2678.
(44) Chavez, L. L.; Onuchic, J. N.; Clementi, C. *J. Am. Chem. Soc.* **2004**, *126*, 8426–8432.
(45) Rea, A. M.; Simpson, E. R.; Meldrum, J. K.; Williams, H. E.; Searle, M. S. *Biochemistry* **2008**, *47*, 12910–12922.
(46) Nymeyer, H. *J. Phys. Chem. B* **2009**, *113*, 8288–8295.
(47) Zheng, W.; Gallicchio, E.; Deng, N.; Andrec, M.; Levy, R. M. *J. Phys. Chem. B* **2011**, *115*, 1512–1523.
(48) Gianni, S.; Brunori, M.; Jemth, P.; Oliveberg, M.; Zhang, M. *Biochemistry* **2009**, *48*, 11825–11830.
(49) Bryngelson, J. D.; Onuchic, J. N.; Socci, N. D.; Wolynes, P. G. *Proteins* **1995**, *21*, 167–195.